Decay and revival dynamics of a quantum state embedded in a regularly spaced band of states

Jan Petter Hansen [*] and Konrad Tywoniuk [†]

Department of Physics and Technology, University of Bergen, 5020 Bergen, Norway

The dynamics of a single quantum state embedded in one continuum or several (quasi)continua is one of the most studied phenomena in quantum mechanics. In this paper we investigate its discrete analog and consider short- and long-time dynamics based on numerical and analytical solutions of the Schrödinger equation. In addition to derivation of explicit conditions for initial exponential decay, it is shown that a recent model of this class [L. Guo, A. Grimsmo, A. F. Kockum, M. Pletyukhov, and G. Johansson, Phys. Rev. A 95, 053821 (2017)], describing a qubit coupled to a phonon reservoir with energy dependent coupling parameters, is identical to a qubit interacting with a finite number of parallel regularly spaced bands of states via constant couplings. As a consequence, the characteristic near periodic initial-state revivals can be viewed as a transition of probability between different continua via the reviving initial state. Furthermore, polynomial decay of the reviving peaks is present in any system with constant and sufficiently strong coupling.

I. INTRODUCTION

The decay dynamics of an unstable or excited quantum state has been one of the most studied topics since the invention of quantum mechanics. Following the pioneering works of Dirac and Landau almost 100 years ago [1,2], Wigner and Weisskopf [3] derived the characteristic Lorentzian line shape of the final-state probabilities assuming exponential decay of the initial state. The constant transition rate derived in the earliest works was later known as Fermi's "golden rule" with reference to his ground-breaking description of nuclear β decay [4]. In the period up till today the number of articles addressing the topic is probably in the order of thousands or more, when counting decay phenomena in subatomic, atomic, molecular, and solid-state physics.

In the time-dependent regime a constant transition rate, as provided by Fermi's "golden rule," immediately leads to an exponential decay law using basic statistics of independent events together with a constant rate [5]. However, there exist numerous cases where nonexponential dynamics is observed, e.g., in Refs. [6–9]. In the most recent experiment [9] an artificial two-level atom is set to interact with acoustic phonon fields with characteristics wavelengths smaller than the atomic dimension, in sharp contrast to "normal" atoms interacting with photon fields. The experiment displayed regular revivals of the initial excited state, i.e., a type of nonexponential dynamics absent in atom-photon decay.

Indeed, the systems where the Hamiltonian provides an exact exponential decay law directly from the time-dependent Schrödinger equation are quite few. The prime example is decay from initial time $t = 0$ up to a fixed time $t + \Delta t$ appearing in a model system with constant coupling from the initial

embedded state to a regularly spaced band of states, sometimes representing a discretized continuum. In its simplest form there is no coupling between band states [10,11]. Thus, the interaction matrix contains nonzero elements on a single row and column which motivates us to refer to this model in the following as the row-column (RC) model [12]. The RC model dates back to the the 1930s and was analyzed by Fano [13] in 1935. Examples of real systems that can be reasonably well described by the RC model are excited atoms or molecules decaying through one-photon transitions to lower states or electron spins interacting with a bath of nuclear spins [14]. Very recently, it was shown that initial exponential decay is a universal phenomenon occurring in a wide range of related many-body systems [15]. It was also shown [16] that harmonic energy dependent coupling parameters result in initial exponential decay of an artificial two-level atom, interacting with surface acoustic phonon states.

An RC model with regularly spaced energy band, with energy separation Δ, reproduces the dynamics of a true continuum as long as the product of the absolute square of the coupling parameter $|\beta|^2$ and density of states Δ^{-1} is kept constant in the limit where $\Delta \to 0$ (Δ itself represents the energy separation between the states in the band, which we assume for now are uniformly distributed). The discrete and the continuum system then reproduce the same physics up to a maximum time $\tau = 2\pi/\Delta$. From then on the dynamics of the discrete system separates from its continuous counterpart. A series of revivals of the initial-state probability occur in the discrete version at times near an integer number of τ. The revival phenomenon of the RC model was initially discussed in Ref. [17] and is also well known in other discrete systems, such as the Jaynes-Cummings model in quantum optics [18].

The origin of the revivals of the RC model can be understood from the fact that the dynamics of the initial state may be transformed into a time delay equation [10]. Each time the system passes through an integer number of τ a

---
*jan.hansen@uib.no
†konrad.tywoniuk@uib.no

new term is added to the amplitude which can cause a partial revival. Alternatively the sequence of imperfect revivals can be understood from the quasiperiodicity which characterizes this particular model when an eigenvector basis is applied. In Ref. [16] it was shown that revivals also occur with harmonic coupling to a true continuum, in sharp contrast to the infinite value of τ for constant coupling. In this case the revivals are occurring at the timescale T of the harmonic modulation of the coupling. The phenomenon was later confirmed in experiments [9].

In this paper we explore the short- and long-time dynamics in the RC model for both types of couplings, constant and harmonic, as well as coupling two distinct bands. The analysis and computations will be based on the eigenvector basis of the full Hamiltonian, which gives a completely analytical expression for the dynamics as long as the energies of the eigenstates are numerically obtained [11,19]. A coherent theoretical analysis, based on the Laplace transform method [12], valid for both coupling types and independent of the inverse density of states, is outlined in parallel. We will show that there exists a close connection between constant couplings to parallel bands and the harmonic coupling to a single continuum. This observation leads to the identification of a long-time power-law decay of revival peaks in the constant-coupling system which is identical to what was discovered in the harmonic case. By simply including an additional dense background reservoir to account for, e.g., noise and temperature fluctuations, we obtain excellent agreement with the experiment [9]. The analysis is carried out in the two following sections, one for each coupling type. The Laplace transform method is provided in the Appendixes. Atomic units are applied throughout.

II. THE RC MODEL WITH CONSTANT COUPLING

Most theoretical methods for solving the Schrödinger equation in a true continuum are based on various analytical methods to obtain a closed form expression of the amplitude describing the embedded decaying initial state. Two classic approaches are the ones of Stey and Gibberd [12], utilizing the Laplace transform, and that of Milonni *et al.* [10], based on the Poisson summation formula. In both cases a delayed time differential equation of the initial amplitude appears. Our approach is based on a discrete representation of the continuum, diagonalizing the Hamiltonian and expressing the initial state in the eigenvector basis. The true continuum dynamics can be obtained when letting the energy separation go to zero in the final expression $\Delta \to 0$ while keeping the ratio $|\beta|^2/\Delta = \text{const}$, where β is the coupling between the singled-out state $a(t)$ and the band. This approach has some advantages since the eigenvector basis is analytical and also numerically available on almost any computer for 10^4 states or more. Computation of time development becomes extremely efficient since only eigenvectors which have a significant overlap with the initial state need to be included in the basis.

A. A single state embedded in a single quasicontinuum

Consider an unstable state $|a, 0\rangle$ with energy ε_a which decays to the ground state with energy ε_b via interactions with a (quasi)continuum. The field free transition frequency

is defined as $\omega_{ab} = \varepsilon_a - \varepsilon_b$. Accompanying the initial state is a vacuum state of the continuum, indicated by the zero in the initial-state ket vector. Correspondingly, the transition to the ground state implies that some of the continuum states are populated by an energy quanta $\varepsilon_n = n\Delta$. For a slow transition only $\varepsilon_n = \omega_{ab}$ gets populated after infinitely long times. For finite transition times many eigenvectors may overlap with the initial state. The state vector describing the complete single-photon (-phonon) transition, $|\Psi(t)\rangle$, is then described by the superposition,

$$|\Psi(t)\rangle = a(t)|a, 0\rangle + \sum_n b_n(t)|g, n\Delta\rangle, \qquad (1)$$

with $a(t)$ and $b_n(t)$ being time-dependent probability amplitudes. By assuming that the state $|a\rangle$ couples with strength β_i only to each of the discretized states and that the latter do not couple between themselves, the time-dependent Schrödinger equation is transformed into a set of N coupled first-order differential equations for the expansion coefficients:

$$i\frac{d}{dt}\begin{pmatrix} a \\ \mathbf{b} \end{pmatrix} = \begin{pmatrix} \omega_{ab} & \mathbf{C}^\dagger \\ \mathbf{C} & \mathbf{\Omega} \end{pmatrix}\begin{pmatrix} a \\ \mathbf{b} \end{pmatrix}. \qquad (2)$$

Here the row vector $\mathbf{b}$ contains the $N - 1$ expansion coefficients $b_n(t)$. The setup is depicted in Fig. 1 (left). The sparse coupling Hamiltonian is Hermitian with nonzero elements defined by the row vector $\mathbf{C}^\dagger = \{\beta_1^*, \beta_2^* ... \beta_{N-1}^*\}$ and the energy levels of the discretized continuum are given by the diagonal matrix, $\mathbf{\Omega} = \text{diag}\{\varepsilon_1, \varepsilon_2 ...\}$. It is straightforward to solve Eq. (2) numerically even for order of thousands to hundreds of thousands of equations. Alternatively, and in general more computationally efficient, we may diagonalize the coupling matrix once, and obtain the time-dependent amplitudes explicitly. The survival amplitude takes the form

$$a(t) = \langle a|\Psi(t)\rangle = \sum_{n=-\infty}^{\infty} |\langle a|v_n\rangle|^2 |v_n\rangle e^{-iE_n t}, \qquad (3)$$

where $|v_n\rangle$ is the nth eigenvector having energy E_n and $a(0) = 1$. The simple structure of the coupling matrix leads to analytical eigenvectors and eigenenergies which can be obtained from a simple implicit equation for each eigenvalue:

$$E_m - \omega_{ab} = \sum_{n=-\infty}^{\infty} \frac{|\beta_n|^2}{E_m - \varepsilon_n}. \qquad (4)$$

As the right-hand side has poles at $E_m = \varepsilon_n$, we obtain exactly one eigenvalue in each interval $(\varepsilon_n, \varepsilon_{n+1})$. Furthermore, the set of energies $E_m - \omega_{ab}$ is symmetrically distributed around ω_{ab}. In the case of an unbounded continuum the effect of the detuning is simply to shift the distribution populated final amplitudes b_n around center eigenvalues from $E_m \sim \omega_{ab}$ to $E_m \approx 0$. Without loss of generality we therefore ignore the detuning in the following. The positive eigenenergies can then be expressed as $E_m = m + \delta_m$ for integer $m \geqslant 0$ and we have $E_{-m} = E_m$ [11]. With the eigenvalues at hand, we obtain the
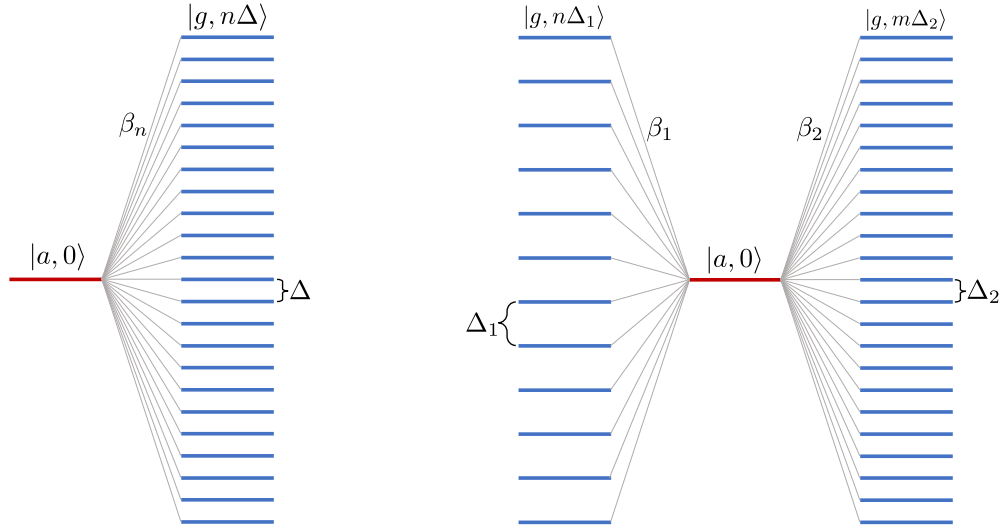
FIG. 1. Schematic presentation of the models studied in this paper. Left: The state $|a, 0\rangle$ embedded in an infinite band of states $|g, n\Delta\rangle$ with band energy separation Δ and coupling β_n. Right: The state $|a, 0\rangle$ embedded in two (or more) bands of states characterized with different band energy separations and constant coupling to each state of the band.

eigenvectors

$$\mathbf{v}_m = \frac{1}{x_m} \begin{pmatrix} 1 \\ \frac{\beta_1}{E_m - \varepsilon_1} \\ \frac{\beta_2}{E_m - \varepsilon_2} \\ \cdot \\ \cdot \\ \cdot \end{pmatrix}, \tag{5}$$

with

$$x_m^2 = 1 + \sum_{j=-\infty}^{\infty} \frac{|\beta_j|^2}{(E_m - \varepsilon_j)^2}. \tag{6}$$

In Ref. [11] it is shown that when all couplings elements are identical, $\beta_j = \beta$ for all j, the summation above can be made, yielding

$$\sum_{j=-\infty}^{\infty} \frac{|\beta|^2}{(E_m - \varepsilon_j)^2} = \left[\frac{\pi\beta}{\Delta \sin\left(\pi \frac{E_m}{\Delta}\right)} \right]^2. \tag{7}$$

It follows that the implicit eigenvalue in Eq. (4) can be written as

$$E_m = \frac{\pi\beta^2}{\Delta \tan\left(\pi \frac{E_m}{\Delta}\right)}. \tag{8}$$

The normalization factor x_m can then be brought to the form

$$x_m^2 = \frac{1}{\beta^2} \left[\beta^2 + \left(\frac{\pi\beta^2}{\Delta}\right)^2 + E_m^2 \right], \tag{9}$$

which leads to a survival probability expressed as

$$a(t) = \sum_{n=1}^{\infty} \frac{2\beta^2}{\beta^2 + (\gamma/2)^2 + E_n^2} \cos(E_n t), \tag{10}$$

where we introduced the rate $\gamma \equiv 2\pi\beta^2/\Delta$.

Exponential decay is obtained in the limit of $\Delta \to 0$ while requiring that the rate γ is kept constant. The first term in the denominator then vanishes and we can take the continuum limit of the sum over band energies. The resulting integral over energy gives exponential decay for all times:

$$a(t) = \frac{\gamma}{\pi} \int_0^{\infty} dE \frac{\cos(Et)}{(\gamma/2)^2 + E^2} = e^{-t\gamma/2}. \tag{11}$$

This corresponds to the Wigner-Weisskopf approximation [3] for our problem and leads to Fermi's "golden rule."

For true discrete systems the replacement of the sum with an integral is less straightforward. The coupling β may well be much larger than γ in Eq. (10) which prohibits the transition to Eq. (11). Thus, one may be lead to the conclusion that the decay dynamics is entirely nonexponential. However, there is always a finite time period $t \in (0, \tau)$, with $\tau \equiv 2\pi/\Delta$, where the decay follows Eq. (11) exactly. Large Δ, or a small rate γ, implies then that the decay is only partial since $|a(\tau)|^2 > 0$.

The proof of the preceding statements is simple: A system with fixed and finite separation between the energy levels can, in the period $t \in (0, \tau)$, be replaced with a factor k denser quasicontinuum. The decay dynamics of both systems are then exactly equal. In the dense band the coupling is given by $\beta_k = \beta/\sqrt{k}$. Since k can be taken arbitrarily large the factor β_k^2 in the denominator eventually vanishes and the validity of the transition from Eq. (10) to Eq. (11) is restored up to $t = \tau$. For $t > \tau$ the dynamics of the original (with spacing Δ) and dense (with spacing Δ_k) systems diverge.

The general amplitude for the embedded state of a true discrete system can now be written in terms of $t = m\tau + t_m$:

$$a(t) = \sum_n \frac{\beta^2}{\beta^2 + \left(\frac{\pi\beta^2}{\Delta}\right)^2 + E_n^2} e^{-im\delta_n \tau} e^{-iE_n t_m}, \tag{12}$$

where $0 < t_m < \tau$. This expression is identical to the solution based on delayed time differential equations below.

In Fig. 2 we display some characteristics of the solution. In the upper panel we observe the characteristics of initial
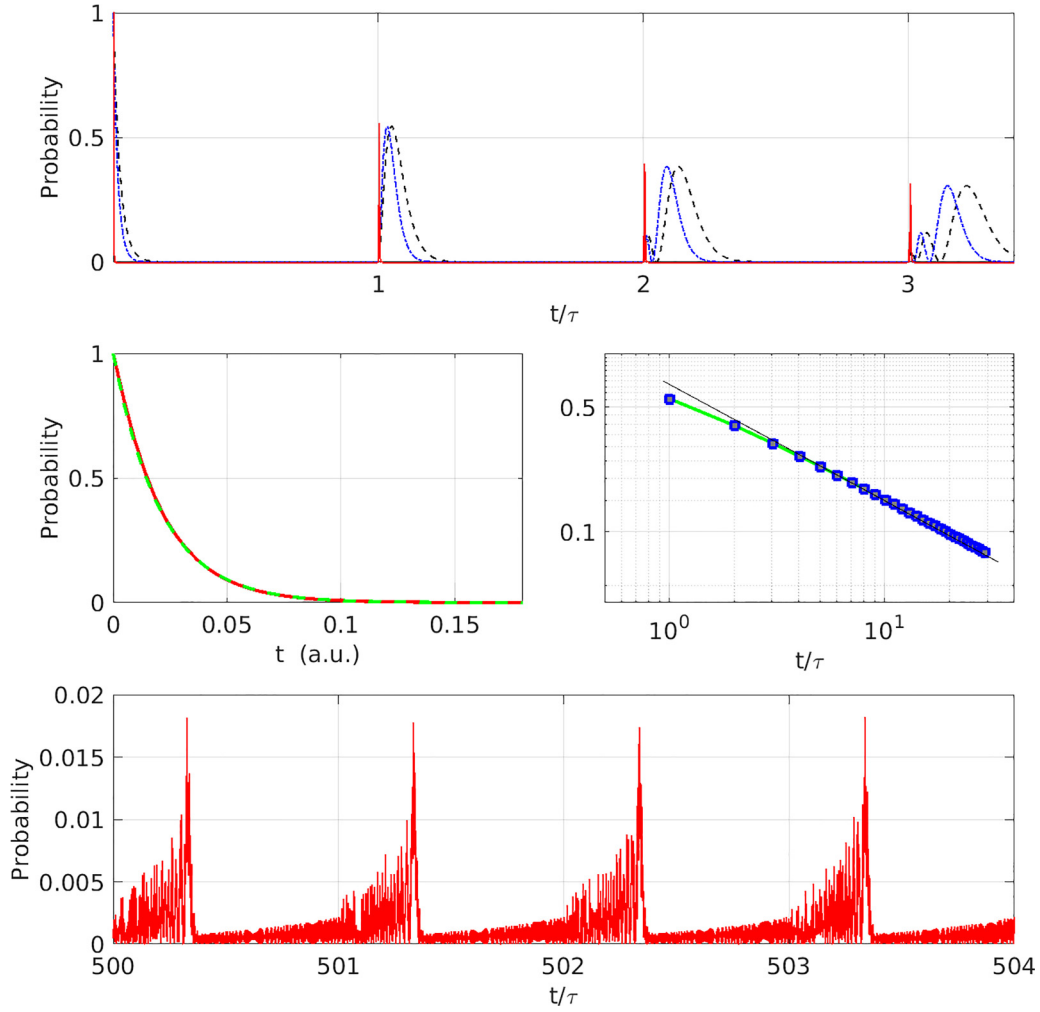
FIG. 2. The upper panel displays the probability for population of the initial state, $|a(t)|^2$, of Eq. (12) for three sets of coupling parameters: $(\beta, \Delta) = (0.0035, 0.035)$ (black dashed curve), $(\beta, \Delta) = (0.2496, 0.2048)$ (blue dash-dotted curve), and $(\beta, \Delta) = (1.2480, 0.2048)$ (red full curve) for a timespan covering the three first revivals. The middle panel shows the exponential decay of the red (dark gray) curve together with the analytical result of Eq. (11) [green (light gray) line to the left]. The right middle panel displays the value of the first 30 revival peaks as blue (dark gray) squares connected by a green (light gray) line. A straight black line is augmented for comparison with exact polynomial decay. The lower panel shows the time development of the red parameter set for a time region after 500 revivals.

dynamics for two different set of coupling parameters and densities of states, both plotted in scaled time units t/τ. The revivals occur initially close to integer times, the height of the peak of the revival probability seems to be independent of the coupling strength, while the "lifetime" of the revival region goes from wide to spikelike as the coupling strength is gradually increased. No matter how large the coupling becomes, the initial decay is always exponential and given by Eq. (11), as illustrated in the middle left panel of Fig. 2. Likewise, collecting the peaks in the strongest-coupling case (red curves) and plotting them in a log-log plot we observe a near polynomial decay for a large number of peaks (from the second revival and outwards in time). Finally, to be discussed below, we plot the dynamics after a large number of revival times (500) in the lowermost panel. Here we see an almost chaotic dynamics building up towards the maximum revival peak. The position of the peak on the time axis has now been clearly shifted beyond the integer numbers (500, 501, etc.) of

τ. At even larger numbers of τ, e.g., 10^4, the signatures of the revivals get more and more blurred and will, due to the true nonperiodicity of the system, never return towards their initial prominence.

In Appendix A, we also derive the time evolution using directly the coupled set of evolution equations and solving them using the Laplace transform. In Appendix A1, we obtain the following solution for the time evolution of state $a(t)$:

$$a(t) = a_0(t) + \sum_{k=1}^{\infty} a_k(t), \tag{13}$$

where $a_0(t) = e^{-t\gamma/2}$, and

$$a_k(t) = -\frac{\gamma t_k}{k} e^{-t_k \gamma/2} L_{k-1}^{\{1\}}(\gamma t_k)\Theta(t_k), \tag{14}$$

where we defined $t_k \equiv t - k\tau$ and $L_n^{\{\alpha\}}(x)$ is the generalized Laguerre function (see also Ref. [12]). In particular, the first terms read

$$a_1(t) = -\gamma(t - \tau)e^{-(t-\tau)\gamma/2}\Theta(t - \tau), \qquad (15)$$

$$a_2(t) = \left[-\gamma(t - 2\tau) + \frac{\gamma^2}{2}(t - 2\tau)^2\right]$$
$$\times e^{-(t-2\tau)\gamma/2}\Theta(t - 2\tau), \qquad (16)$$

$$a_3(t) = \left[-\gamma(t - 3\tau) + \gamma^2(t - 3\tau)^2 - \frac{\gamma^3}{6}(t - 3\tau)^3\right]$$
$$\times e^{-(t-3\tau)\gamma/2}\Theta(t - 3\tau). \qquad (17)$$

At first look, it seems sufficient to demand that

$$\tau\gamma/2 \gg 1, \qquad (18)$$

in order to ensure that each term decays sufficiently fast, and in the step $n\tau < t < (n+1)\tau$ it is only the nth term that contributes. We will assume this condition is fulfilled in the following discussion.

The first contribution $a_1(t)$, that breaks with the exponential decay behavior, sets in at times $\tau < t < 2\tau$, and reaches a peak value at $t = \tau + 2/\gamma$. Here, the probability peaks at $4/e^2 \approx 0.54$. In the second interval, $2\tau < t < 3\tau$, $a_2(t)$ starts contributing, leading to two peaks at times $t = 2\tau + (3 \pm \sqrt{5})/\gamma$. At these positions, the probability peaks at $\{4(2 - \sqrt{5})^2 e^{-3+\sqrt{5}}, 4(2 + \sqrt{5})^2 e^{-3-\sqrt{5}}\} \approx \{0.10, 0.38\}$, respectively. Hence, the smaller peak precedes the bigger one. Similarly, in the third interval, $3\tau < t < 4\tau$, there are three peaks and so on.

There are several features worth pointing out. First, while the positions of the peaks clearly depend on τ and γ, the heights of the peaks are completely independent of the parameters of the model. Second, at late times the multiple peaks that occur force the largest, and also latest, peak to be displaced so that ultimately the condition $\tau\gamma/2 \gg 1$ is not sufficient to ensure that only one contribution from the sum contributes in a certain time interval. This "leakage" effect inevitable leads to a chaotic behavior at late times, as can be inferred from the bottom panel of Fig. 2.

B. Two and more parallel bands of states

In nature, several deexcitation processes occur in the presence of competing and separable continua such as Auger versus radiative decay processes in atomic physics. The problem was treated by Fano in 1961 [20] for real continua. Here we consider the dynamics for parallel energy bands with focus on the total system behavior when the involved continua have different isolated revival times. Within the RC model, two continua in their simplest form have two different constant coupling parameters, β_1 and β_2, and/or inverse densities of states Δ_1 and Δ_2. No direct coupling between the bands is taken into account, nor is coupling between states belonging to the same band due to interaction with the initial state. This setup is depicted in Fig. 1 (right). The dynamics is now

described by the expansion

$$|\Psi(t)\rangle = a(t)|a\rangle + \sum_n b_n(t)|g, n\Delta_1\rangle + \sum_m c_n(t)|g, m\Delta_2\rangle. \qquad (19)$$

Without loss of generality, again we neglect the effect of detuning. Projecting out on each basis vector we obtain a coupling matrix which has the same structure as in the case of a single continuum:

$$i\frac{d}{dt}\begin{pmatrix} a \\ \mathbf{b} \\ \mathbf{c} \end{pmatrix} = \begin{pmatrix} \omega_{ab} & \mathbf{C}_1^\dagger & \mathbf{C}_2^\dagger \\ \mathbf{C}_1 & \mathbf{\Omega_1} & \mathbf{0} \\ \mathbf{C}_2 & \mathbf{0}^\dagger & \mathbf{\Omega_2} \end{pmatrix}\begin{pmatrix} a \\ \mathbf{b} \\ \mathbf{c} \end{pmatrix}, \qquad (20)$$

where again the amplitudes and coupling to the bands have been expressed as vectors $\mathbf{b}$, $\mathbf{c}$. The matrices $\mathbf{\Omega_{1,2}}$ contains the discrete band energy levels on the diagonal, $\mathbf{\Omega}_{1,2}^{n,m} = \delta_{n,m}n \cdot \Delta_{1,2}$. Finally the matrix $\mathbf{0}$ contains only zeros since the two continua do not interact directly.

The implicit equation for the eigenvalues now becomes

$$E_m = |\beta_1|^2 \sum_n \frac{1}{E_m - n\Delta_1} + |\beta_2|^2 \sum_k \frac{1}{E_m - k\Delta_2}. \qquad (21)$$

To obtain the decay dynamics, consider the case when $\Delta_2 > \Delta_1$ and replace this continuum with one which has the same energy separation as the first, i.e., Δ_1. This implies a reduced coupling strength in the replacement band $\hat{\beta}_2 = \beta_2\sqrt{\Delta_1/\Delta_2}$. The new implicit equation for eigenvalues then takes the form

$$E_m = (|\beta_1|^2 + |\hat{\beta}_2|^2) \sum_{n=-\infty}^{\infty} \frac{1}{E_m - n\Delta_1}. \qquad (22)$$

As remarked by Fano [20], this leaves us with exactly the same identities Eqs. (4)–(11). Therefore, the obtained exponential decay of the initial channel becomes

$$P_a(t) = e^{-\gamma_{12}t}, \qquad (23)$$

at early times, where the rate constant

$$\frac{\gamma_{12}}{2} = \pi \frac{|\beta_1|^2 + |\hat{\beta}_2|^2}{\Delta_1} = \pi\left(\frac{|\beta_1|^2}{\Delta_1} + \frac{|\beta_2|^2}{\Delta_2}\right). \qquad (24)$$

Each band becomes initially populated according to a weighted fraction:

$$P_i(t) = \frac{\gamma_i}{\gamma_{12}}(1 - e^{-\gamma_{12}t}) \qquad (25)$$

where $P_i(t)$ $(i = 1, 2)$ is the total probability summed over the total, in principle infinite, number of states within band i and $\gamma_i = 2\pi|\beta_i|^2/\Delta_i$ (for further details see Appendix B).

Exponential decay is now limited to the period $t \in (0, \min[\tau_1, \tau_2])$, where $\tau_i = 2\pi/\Delta_i$. For integer revival periods of τ_1, τ_2 we will expect the system to undergo a backcoupling of probability to the initial state as long as the band in question is not empty. In Appendix B we have solved the analytical case of two continua. In the strong-coupling region an infinite set of additional revival times occurs, namely, at integer intervals of $\tau_1 + \tau_2$, as well as arbitrary multiples of the two, i.e., $n\tau_1 + m\tau_2$, where $n, m > 1$ and $n \neq m$.
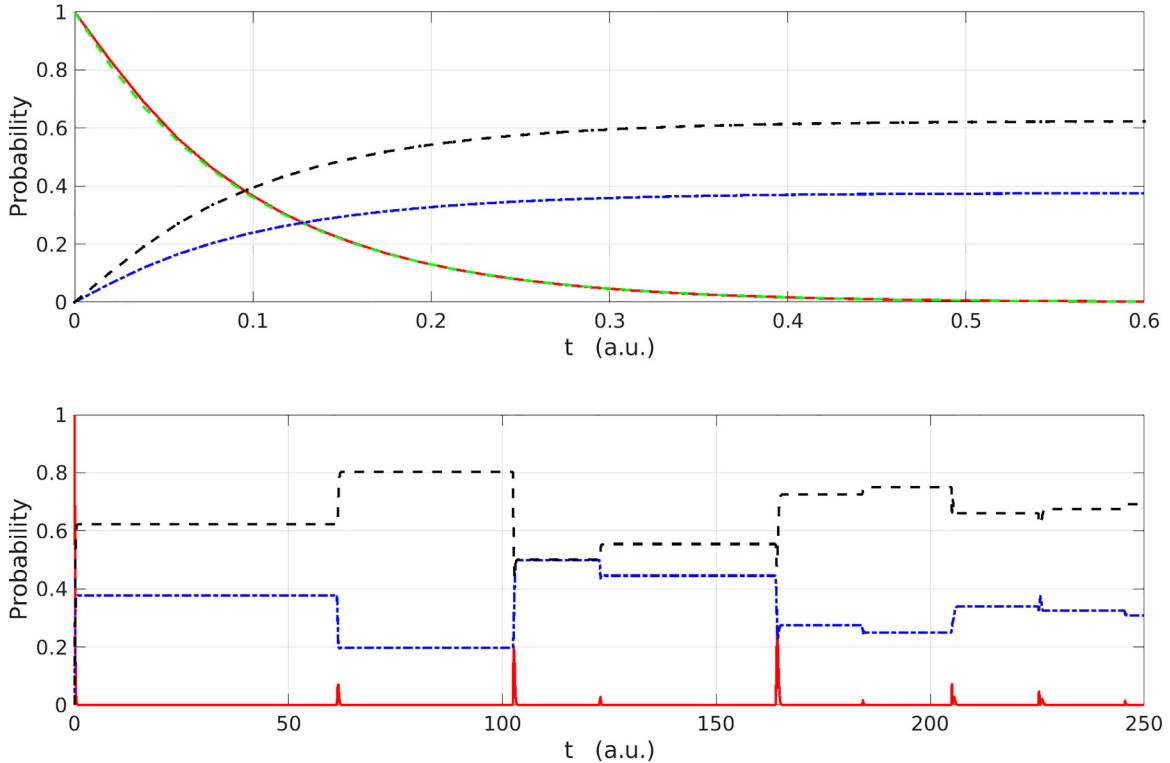
FIG. 3. Exponential decay and total population probability for two continua coupled to the initial state with the same coupling parameter $\beta = 0.2496$. The continuum represented with the blue (dash-dotted) line has an energy separation $\Delta_1 = 0.1024$ ($\tau_1 = 61.36$) while the other (black dashed) line has $\Delta_1 = 0.0613$ ($\tau_2 = 102.5$). The upper panel shows the short-time dynamics with the analytical exponential decay solution in dashed green (light gray) and the red line (dark gray) is the numerical one. The lower panels display the long-time dynamics.

Another striking feature is that the heights of the revival peaks now depend on the ratio of the rates γ_1/γ_2. This is in contrast to the case of constant coupling, and harmonic as we will discuss below, where the height of the peak is completely determined by the "structure" of the system while the peaks do not depend on the rate. For further details see Appendix B. In other words, the heights of the peaks can be tuned by the rates γ_i, and the revival times are given by τ_i [21]

In Fig. 3 we display an example. The upper panel shows the exponential decay into two different continua at short times. The lower panel shows the redistribution dynamics of probability at long timescales, first from the "blue" continuum to the "black," since the blue ban has the shorter revival time. The transfer of probability takes place via the initial state manifesting itself as a transient revival of that state accompanying each partial revival. In the figure the first (blue) revival takes place around $t = 61$ a.u., and the second (black) revival takes place around $t = 102$ a.u. At $t = 2 \times 61$ a.u. we see a weak signature in the initial state of the second blue revival time and then around $t = 161$ we observe a strong new revival at $t = \tau_1 + \tau 2$, as expected. At increasing integer number of linear combinations of the two isolated revival times the two continua interchange probability each time, and each interchange implies, on this timescale and coupling parameter, a spikelike repopulation of the initial state.

Both methods can be directly expanded to describe more than two parallel bands, which in general will display even more complex dynamics as long as the revival times of each band differ.

III. HARMONIC COUPLING

Another class of atom-field couplings is the class of coupling parameters which are periodic. The periodicity can originate from partial reflection of the radiation emitted from an excited atom, where the partially reflected part at some later time interferes with a later emitted radiation which is unreflected [22]. Another example is a qubit connected to a substrate at two points separated a distance $2L$. The coupling from the two-level system to the surface plasmon states was recently analyzed in detail [16]. Writing $\beta_n = \beta \cos(n\Delta T/2)$, in the continuum limit one can derive an elegant solution, which in our notation reads

$$a(t) = \sum_{n=0}^{\infty} \frac{\left[-\frac{\gamma}{4}(t - nT)\right]^n}{n!} e^{-(t-nT)\gamma/4} \Theta(t - nT), \quad (26)$$

where we again have chosen $a(0) = 1$ and neglected the detuning energy. This structure is considerably simpler than the one for a constant coupling [see Eqs. (13) and (14)]. In particular, note the absence of multiple peaks at later revival times $t > nT$ [23]. In order to address this "simplicity," we set out to analyze specific cases when the band densities, concretely $2\pi/\Delta$, are multiples of the modulation timescale T.

We now address the dynamics using the discrete basis eigenvector approach. Consider Eq. (2) and replace the constant coupling parameter β with an energy dependent coupling $\beta_n = \beta \cos(n\Delta T/2)$. In the analysis in Ref. [16], the period T is related to the distance L between two contact points

between the qubit and the substrate, $T = L/v_g$ where v_g is the speed of sound in the acoustic medium. By defining symmetric and antisymmetric discrete phonon states from the basis applied in Ref. [16], only the symmetric ones couple to the qubit and we arrive at our Eq. (2). The eigenstates are then given by the sum of Eq. (4). Let us rewrite the sum in terms of

$$\mathcal{S} = \sum_{n=-\infty}^{\infty} \frac{\left| \beta \cos\left(n\Delta T/2 \right) \right|^2}{E - \Delta n}. \tag{27}$$

A general solution can be found using special functions. Here, we consider a few illustrative cases, using increasingly smaller energy separation between the discrete states.

(a) $\Delta = 2\pi/T$: This is equivalent to a constant coupling $\beta_n = \beta$ to all the energy levels. The answer is

$$\frac{\Delta}{\beta^2} \mathcal{S} = \frac{\pi}{\tan[\pi z]}, \tag{28}$$

where $z = E/\Delta$. Further discussion can be found in Sec. II A.

(b) $\Delta = \pi/T$: The constant coupling β is modulated by the following possible values $\cos(\omega_n T/2) = \{1, 0, -1, \ldots\}$ for $n = \{0, 1, 2, \ldots\}$, etc. The sum therefore becomes

$$\frac{\Delta}{\beta^2} \mathcal{S} = \sum_{n=-\infty}^{\infty} \frac{1}{z - 2n} = \frac{\pi}{2 \tan\left[\frac{\pi}{2} z\right]}. \tag{29}$$

This is equivalent to a constant coupling $\beta_n = \beta$ to all the energy levels. This choice of Δ gives the correct exponential decay up to $t = T$ with a decay rate constant half the magnitude of the decay constant of Eq. (11), namely, $\gamma' = \frac{\pi \beta^2}{\Delta} = \gamma/2$. Further discussion can be found in Appendix A2.

At $t = T$ the backcoupling to the initial state departs from the correct continuum behavior. From Eq. (15), we find a first peak at $t_1 = T + 4/\gamma$ reaching $P(t_1) = 4/e^2$. This is a factor 4 too large compared to the continuum solution from Eq. (26). Obviously, the multiple peaks associated with revivals at $t > 2T$, discussed in detail in Sec. II A, are also not present in the continuum limit.

(a) $\Delta = 2\pi/(3T)$: The constant coupling β is now modulated by the following possible values $\cos(\omega_n T/2) = \{1, \frac{1}{2}, -\frac{1}{2}, \ldots\}$ for $n = \{0, 1, 2, \ldots\}$. The sum therefore becomes

$$\frac{\Delta}{\beta^2} \mathcal{S} = \sum_{n=-\infty}^{\infty} \frac{1}{z - 3n}$$
$$+ \frac{1}{4} \sum_{n=-\infty}^{\infty} \left[\frac{1}{z - (3n - 1)} + \frac{1}{z - (3n + 1)} \right]$$
$$= \frac{\pi}{3 \tan\left[\frac{\pi}{3} z\right]} - \frac{\pi}{3} \frac{\sin\left[\frac{2\pi}{3} z\right]}{1 + 2 \cos\left[\frac{2\pi}{3} z\right]}. \tag{30}$$

This representation describes the dynamics up to the revival time $t = 2T$. The couplings and energy levels of the discrete states distribute themselves in what can be viewed as parallel continua: The first one has coupling strength and energy separation $|\beta, 3\Delta|$; the second has $|\beta/2, \Delta|$, in addition making sure that the overlapping levels are not occupied twice.

We have worked out this case in detail up to times $t \leqslant 3T$ in Appendix A3. For the time interval $0 < t < 2T$, we find

that

$$a(t) = e^{-t\gamma/4} - \frac{\gamma}{4}(t - T)e^{-(t-T)\gamma/4}\Theta(t - T). \tag{31}$$

At the first revival at $t = T$, the peak position remains at $T + 4/\gamma$, but now the height is reduced to $P = 1/e^2$, which is in agreement with the continuum result in Eq. (26). Strikingly, as for the case of constant coupling to a single (quasi) continuous band in Sec. II A, the height of the first peak is completely independent of the coupling or level density spacing. This also holds for the subsequent peaks. Only their positions are occurring at intervals $nT + c/\gamma$, where c is a number describing the positions of the multiple peaks. However, at $t \geqslant 3T$ this model starts exhibiting multiple peaks and, thus, does not agree anymore with the continuum solution (26), so we will not discuss it further here.

(b) $\Delta = \pi/(2T)$: The constant coupling β is now modulated by the following possible values $u \cos(\omega_n T/2) = \{1, \frac{1}{\sqrt{2}}, 0, \ldots\}$ for $n = \{0, 1, 2, \ldots\}$, etc. The sum therefore becomes

$$\frac{\Delta}{\beta^2} \mathcal{S} = \sum_{n=-\infty}^{\infty} \frac{1}{z - 4n}$$
$$+ \frac{1}{2} \sum_{n=-\infty}^{\infty} \left[\frac{1}{z - (4n - 1)} + \frac{1}{z - (4n + 1)} \right],$$
$$= \frac{\pi}{4 \tan\left[\frac{\pi}{4} z\right]} - \frac{\pi}{4} \tan\left[\frac{\pi}{2} z\right]. \tag{32}$$

Again this is effectively two parallel continua, avoiding any overlaps, now with parameters $|\beta, 4\Delta|$ and $|\beta/2, \Delta|$. We have worked out this case in detail in Appendix A4.

This particular discretization gives identical population in the two continua up to $t = T$ and the redistribution gives the correct dynamics of the initial state up to $t = 3T$. Since up to $t = 2T$ the result is exactly the same as in the previous cases, let us only write out the additional piece that appears at $t > 2T$, namely,

$$a^{(2)}(t) = \frac{\gamma^2}{32}(t - 2T)^2 e^{-(t-2T)\gamma/4}\Theta(t - 2T). \tag{33}$$

Now, there is only one peak in the interval $2T < t < 3T$, located at $t_2 = 2T + \frac{8}{\gamma}$, where the probability peaks at $P(t_2) = 4/e^4 \approx 0.073$. The agreement with the continuum result now extends to $t < 3T$. Again, the height of the second peak does not depend on the parameters of the model.

In summary, the dynamics of the qubit with harmonic coupling to a substrate can alternative be viewed as the dynamics of a series of parallel continua with different constant coupling and density of states. At least one parallel continuum has a revival at an integer number of T which causes backcoupling to the initial state followed by a redistribution of the population probability of each quasicontinuum. The dynamics described above is illustrated in Fig. 4.

By taking a sufficiently small Δ we can effectively simulate the dynamics for arbitrarily large times. In Fig. 5 this is done for a case which has $\tau \approx 19T$. A large number of initial-state revivals is seen up to the point $t = \tau$ where *all* parallel continua have a backcoupling to the initial state. As a consequence this peak is much larger than the partial revivals
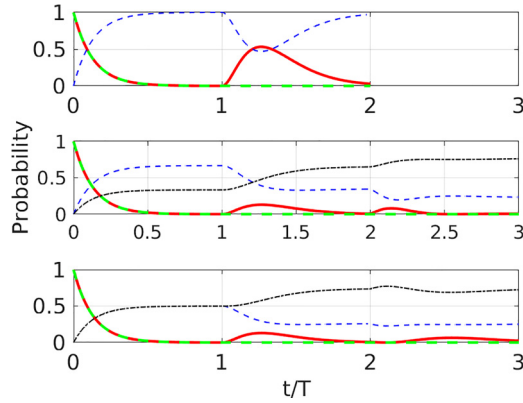
FIG. 4. Dynamics of the initial qubit state (red full line) and parallel "phonon continua" (dashed blue line and black dash-dotted line) for varying energy separation, $\Delta = 2\pi/(MT)$. Upper panel, $M = 2$; middle panel, $M = 3$; lower panel, $M = 4$. The thick broken green (dark gray) curved line is the analytical initial exponential decay. The red (light gray) line in the lowest panel is identical with the exact result (see Ref. [16]).

at integer values of t/T. In the lower left panels the initial decay at very short time again is observed, and in full agreement with the analytical decay rate constant. Finally, as also shown in the case of constant coupling, the revival peaks display a polynomial decay up to $t = \tau$.

The use of discrete parallel continua makes it simple to model experiments as well, for example in the case of Ref. [9] where a number of other couplings appear due to temperature fluctuations or other conditions related to the experiment. By simply augmenting the discrete model ($M = 4$) with a dense reservoir which on the timescale of the experiment does not
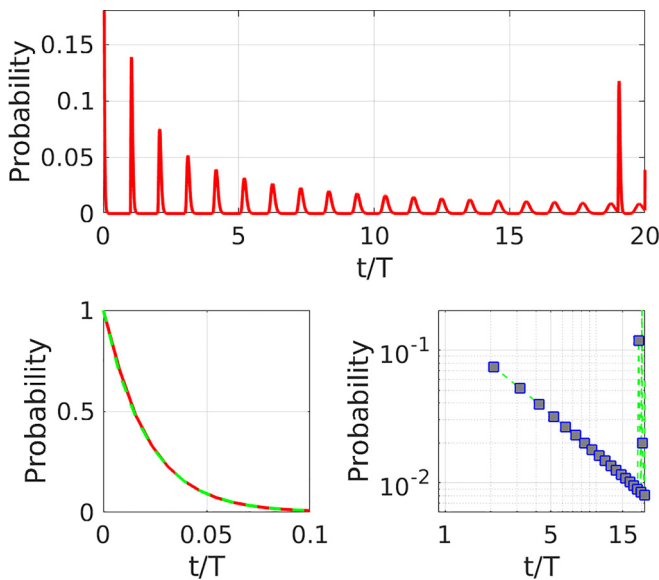

FIG. 5. The upper panel shows the probability of the initial state in a simulation with 7000 states in total. Parameters: $T = 1$, $\Delta = 2\pi/(MT)$, $M = 20$, and $\beta = 2.1859$. The lower left panel shows the simulated and analytical initial time developments of the initial-state probability and the lower right panel displays the peak values of the initial-state revivals.
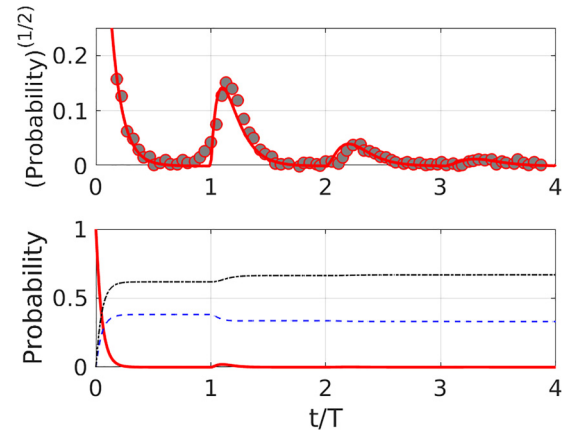

FIG. 6. The upper panel shows the absolute amplitude of the initial state in a simulation with 1000 states compared with the experimental results (circles) in Ref. [9]. Parameters: $T = 4$, $\Delta = 2\pi/(MT)$, $M = 20$, and $\beta = 0.4372$. In addition a "heat reservoir" described by 5000 states and a factor 5 denser energy separation, $\Delta_{\text{heat}} = \Delta/5$, has been added. The coupling from the excited qubit state to the heat reservoir is $\beta_{\text{heat}} = 0.176$. The lower panel shows the time-dependent probability distributions of the excited qubit state (red thick line), summed phonon [blue (dark gray) dashed line], and reservoir state (black dashed line).

undergo any revivals we can simulate a leak of probability due to heat. The result, shown in Fig. 6, is in excellent agreement with experimental data from Ref. [9].

IV. CONCLUDING REMARKS

In this paper we have considered the dynamics of a quantum model which goes back almost to the invention of quantum mechanics. Inspired by the recent progress and application of the model relevant for qubit dynamics of modern quantum computers, we analyzed the general problem based on a single state interacting with one or several discrete band(s). The analysis was performed in an eigenvector basis and with a complementary analytical method applicable to real as well as discrete "continua."

A number of properties were identified, in particular, the following.

(i) A discrete band of states implies well-defined revival peaks. For a single band the heights of the peaks are independent of coupling strengths and the peak strengths show near polynomial decays on a time interval covering several tens of revival times.

(ii) The qubit dynamics with harmonic couplings between the initial state and a true (phonon) continuum is identical to a qubit coupled by constant factors to a number of parallel bands. Revivals in the latter model are understood as a transient population flow through the initial state and between different bands.

(iii) Comparison with experiments based on the numerical approach was straightforward and in excellent overall agreement.

The present approach opens the way for direct modeling of time-dependent scattering phenomena due to point contacts, time induced multiphonon (photon) processes, and a num-

ber of other phenomena relevant for the long research path towards the realization of stable and effective working quantum computers.

APPENDIX A: LAPLACE TRANSFORM METHOD

The quantum evolution described above can also be cast as a system of evolution equations for the state $a(t)$ coupled to a quasicontinuum $b_n(t)$:

$$\dot{a}(t) = -i \sum_{n=-\infty}^{\infty} \beta_n b_n(t), \tag{A1}$$

$$\dot{b}_n(t) = -i\omega_n b_n(t) - i\beta_n^* a(t), \tag{A2}$$

where $\omega_n = n\Delta$, and Δ is the level spacing of the quasicontinuum. Integrating out the second equation, yielding

$$b_n(t) = -i\beta_n \int_0^t dt' \, e^{-i\omega_n(t-t')} a(t'), \tag{A3}$$

and inserting the solution into the first, we obtain the standard solution

$$\dot{a}(t) = -\int_0^t dt' \, a(t') \sum_{n=-\infty}^{\infty} |\beta_n|^2 e^{-i\omega_n(t-t')}. \tag{A4}$$

This has the form of a delay differential equation [10].

Instead, we will be interested in keeping a finite $\Delta > 0$ and studying the set of discrete modes. This problem can be solved in Laplace space, where the Laplace transform of $a(t)$, defined as

$$\tilde{a}(s) = \int_0^\infty dt \, e^{-st} a(t), \tag{A5}$$

is given by

$$\tilde{a}(s) = \frac{a(0)}{s + \Pi(s)}, \tag{A6}$$

where $\Pi(s) = i \sum_{n=-\infty}^{\infty} \frac{|\beta_n|^2}{is - \omega_n} = i\mathcal{S}(is)$. Note that $\Pi(-s) = -\Pi(s)$. The inverse transform, defined as

$$a(t) = \int_C \frac{ds}{2\pi i} e^{st} \tilde{a}(s), \tag{A7}$$

where the contour C runs along the imaginary axis to the right of any poles of $\tilde{a}(s)$, then becomes sensitive to the poles of $\tilde{a}(s)$. These are found by solving

$$s + \Pi(s) = 0. \tag{A8}$$

By identifying $is \leftrightarrow E$, the pole structure is equivalent to the eigenvalue equations.

1. Constant coupling

As mentioned above, a constant coupling is equivalent to setting the level spacing $\Delta = 2\pi/T$ in the harmonic coupling. Using the sum derived in (28), we find

$$\Pi(s) = i\frac{\gamma}{2} \cot(i\ell s) = \frac{\gamma}{2} \coth(\ell s), \tag{A9}$$

where $\gamma = 2\pi\beta^2/\Delta$ and $\ell = \pi/\Delta$. In order to introduce the techniques to inverse the Laplace transform [12], we will review this case in detail.

It is possible to rewrite as

$$\tilde{a}(s) = \frac{1 - e^{-2\ell s}}{s + \gamma/2} \left[1 - \frac{s - \gamma/2}{s + \gamma/2} e^{-2\ell s} \right]^{-1}. \tag{A10}$$

Since $|(s - \gamma/2)/(s + \gamma/2)e^{-2\ell s}| < 1$ for sufficiently large ℓ, or small Δ, we can expand the last term as an infinite series $(1 - x)^{-1} = \sum_{n=0}^{\infty} x^n$. Then, after further manipulations, we write the whole expression as

$$\tilde{a}(s) = \frac{1}{s + \gamma/2} - \gamma \sum_{k=1}^{\infty} \frac{(s - \gamma/2)^{k-1}}{(s + \gamma/2)^{k+1}} e^{-2k\ell s}. \tag{A11}$$

This demonstrates that there is only one location of the poles, i.e., at $s_* = -\gamma/2$. We can therefore safely let the contour C run along the origin of the complex s plane, i.e., $s = i\xi$ with $\xi \in [-\infty, \infty]$ with a counterclockwise circle at infinity. Define

$$a(t) = a_0(t) + \sum_{k=1}^{\infty} a_k(t), \tag{A12}$$

where

$$a_0(t) = \int_C \frac{ds}{2\pi i} \frac{e^{st}}{s + \gamma/2} = e^{-t\gamma/2}, \tag{A13}$$

and

$$a_k(t) = \int_C \frac{ds}{2\pi i} \tilde{a}_k(s) e^{st}, \tag{A14}$$

with $\tilde{a}_k(s) = -\gamma \frac{(s-\gamma/2)^{k-1}}{(s+\gamma/2)^{k+1}} e^{-2k\ell s}$. The coefficients $a_k(t)$ can easily be found using the residue theorem,

$$a_k(t) = \frac{1}{k!} \lim_{s \to s_*} \frac{d^k}{ds^k} \left[(s + \gamma/2)^{k+1} \tilde{a}_k(s) e^{st} \right], \tag{A15}$$

as long as the function decays fast enough on the circle at infinity, in this case as long as $t > 2k\ell s$. We use the binomial formula to write

$$\frac{d^k}{ds^k} \left[(s - \gamma/2)^{k-1} e^{(t-2k\ell)s} \right]$$

$$= \sum_{n=0}^{k-1} \frac{(k-1)!}{(k-1-n)!} (s - \gamma/2)^{k-1-n} (t - 2k\ell)^{k-n} e^{(t-2k\ell)s}. \tag{A16}$$

Finally, after further manipulations, we can recast the answer as

$$a_k(t) = -\frac{\gamma(t - k\tau)}{k} e^{-(t-k\tau)\gamma/2} L_{k-1}^{\{1\}}[\gamma(t - k\tau)] \Theta(t - k\tau), \tag{A17}$$

where we defined $\tau = 2\pi/\Delta$ and $L_n^{\{\alpha\}}(x)$ is the generalized Laguerre function. Note that in this case we have exactly that $\tau = T$.

The occupation of the continuum states is found from Eq. (A3). For instance, up to the first revival time, i.e., $0 < t < \tau$, where $P_a(t) = e^{-t\gamma}$, the solution is

$$b_n(t) = \frac{i\beta}{\frac{\gamma}{2} - in\Delta}(e^{-t\gamma/2} - e^{-in\Delta t}). \tag{A18}$$

The probability for the whole continuum then becomes

$$P_b(t) = \sum_{n=-\infty}^{\infty} |b_n(t)|^2. \tag{A19}$$

To prove that the total probability is conserved, we use the following identities:

$$\sum_{n=-\infty}^{\infty} \frac{1}{z^2 + n^2} = \frac{\pi}{z} \coth(z\pi), \tag{A20}$$

$$\sum_{n=-\infty}^{\infty} \frac{\cos(xn)}{z^2 + n^2} = \frac{\pi}{z} \frac{\cosh[z(\pi - x)]}{\sinh(z\pi)}, \tag{A21}$$

for $0 < x < 2\pi$ [24], to derive that

$$P_b(t) = 1 - e^{-t\gamma}. \tag{A22}$$

This demonstrates that $P_a(t) + P_b(t) = 1$, as expected.

2. Harmonic coupling with $\Delta = \pi/T$

Using (29) to obtain that

$$\Pi(s) = \frac{\gamma}{4} \coth\left(\frac{\ell s}{2}\right), \tag{A23}$$

we realize that the pole structure and therefore also the inverse Laplace transform are completely equivalent to the previous case with the replacement $\gamma \to \gamma/2$ and the explicit mapping of $\tau \to T$. The first correction therefore reads

$$a_1(t) = -\frac{\gamma}{2}(t - T)e^{-(t-T)\gamma/4}\Theta(t - T), \tag{A24}$$

in this case. Further terms, appearing at $t > 2T$, can be found directly from previous formulas.

3. Harmonic coupling with $\Delta = 2\pi/(3T)$

In this case, with the help of (30), we found

$$\Pi(s) = \frac{\gamma}{6} \coth\left(\frac{\ell s}{3}\right) + \frac{\gamma}{6} \frac{\sinh\left(\frac{2}{3}\ell s\right)}{1 + 2\cosh\left(\frac{2}{3}\ell s\right)}. \tag{A25}$$

Following the same line of arguments as before, and introducing the shorthand $y \equiv e^{-\frac{2}{3}\ell s}$, we find that

$$\tilde{a}(s) = \frac{1 - y^3}{s + \gamma/4}\left[1 - \frac{(s - \gamma/4)y^3 - (y + y^2)\gamma/4}{s + \gamma/4}\right]^{-1}. \tag{A26}$$

After further manipulations, we arrive at

$$\tilde{a}(s) = \frac{1}{s + \gamma/4} - \frac{\gamma}{2}\sum_{k=1}^{\infty} \frac{[(s - \gamma/4)y^3 - (y + y^2)\gamma/4]^{k-1}}{(s + \gamma/4)^{k+1}}$$

$$\times (y^3 + y^2/2 + y/2). \tag{A27}$$

We identify the emerging multiple poles at $s = s_* = -\gamma/4$, however the structure of the numerator is much more complicated. It is possible to proceed further by expanding the numerator by using the binomial formula, but we will not proceed further.

Instead, let us first have a look at the first term in the expansion in (A27), which reads

$$\tilde{a}_1(s) = -\frac{\gamma}{2} \frac{e^{-3Ts} + e^{-2Ts}/2 + e^{-Ts}/2}{(s + \gamma/4)^2}. \tag{A28}$$

The three terms in the denominator will contribute to the evolution only at $t > 3T$, $t > 2T$, and $t > T$, respectively. Similarly, $\tilde{a}_2(s)$ will contain terms that contribute at subsequent time intervals, starting at $t > 2T$ and up to $t > 6T$. We will currently only be interested in the terms that describe the evolution in the interval $0 < t < 3T$. The contribution that starts to contribute at times $nT < t$, we will denote $a^{(n)}(t)$. Naturally, $a^{(0)}(t) = e^{-t\gamma/4}$ from the single pole contribution.

Focusing now on the next interval, $T < t < 2T$, we note that only $\tilde{a}_1(s)$ contributes. We find

$$a^{(1)}(t) = -\frac{\gamma}{4}\int_C \frac{ds}{2\pi i} \frac{e^{(t-T)s}}{(s + \gamma/4)^2}$$

$$= -\frac{\gamma}{4}(t - T)e^{-(t-T)\gamma/4}\Theta(t - T). \tag{A29}$$

This piece reaches a maximal value at $t = T + 2/\gamma$, as before, where the contribution to the probability reaches a maximal value of $e^{-2} \approx 0.14$. This is a factor 4 smaller than in the previous cases.

The additional contribution in the next piece, i.e., $t > 2T$, receives contributions from both $\tilde{a}_1(s)$ and $\tilde{a}_2(s)$. We find

$$a^{(2)}(t) = -\frac{\gamma}{4}\int_C \frac{ds}{2\pi i} \frac{e^{(t-2T)s}}{(s + \gamma/4)^2} + \frac{\gamma^2}{16}\int_C \frac{ds}{2\pi i} \frac{e^{(t-2T)s}}{(s + \gamma/4)^3},$$

$$= \left[\left(-\frac{\gamma}{4}\right)(t - 2T) + \frac{\gamma^2}{32}(t - 2T)^2\right]$$

$$\times e^{-(t-2T)\gamma/4}\Theta(t - 2T). \tag{A30}$$

There are two maxima at $t = 2T + \frac{4}{\gamma}(2 \mp \sqrt{2})$, corresponding to peak values on the level of the probability that are $\{(3 - 2\sqrt{2})e^{-4+2\sqrt{2}}, (3 + 2\sqrt{2})e^{-4-2\sqrt{2}}\} \approx \{0.053, 0.006\}$.

Compared to the continuum limit, $\Delta \to 0$, we find agreement of the height of the peak in the interval $T < t < 2T$. The multiple peaks occurring at later times are also not present in the $\Delta \to 0$ solution.

4. Harmonic coupling with $\Delta = \pi/(2T)$

In this case, from Eq. (32), we have

$$\Pi(s) = \frac{\gamma}{8} \coth\left(\frac{\ell s}{4}\right) + \frac{\gamma}{8} \tanh\left(\frac{\ell s}{2}\right). \tag{A31}$$

After standard manipulations, we arrive at

$$\tilde{a}(s) = \frac{1}{s + \gamma/4} - \frac{\gamma}{2}\sum_{k=1}^{\infty} \frac{[(s - \gamma/4)y^3 + (y - y^2)s]^{k-1}}{(s + \gamma/4)^{k+1}}$$

$$\times (y^3 - y^2/2 + y/2). \tag{A32}$$

Proceeding as before, we find the following behavior for the early-time evolution:

$$a^{(1)}(t) = -\frac{\gamma}{4}(t - T)e^{-(t-T)\gamma/4}\Theta(t - T), \quad (A33)$$

$$a^{(2)}(t) = \frac{\gamma^2}{32}(t - 2T)^2 e^{-(t-2T)\gamma/4}\Theta(t - 2T). \quad (A34)$$

Now, there is only one peak in the interval $2T < t < 3T$, located at $t = 2T + \frac{8}{\gamma}$, where the probability peaks at $4/e^4 \approx 0.073$. The agreement with the continuum result now extends to $t < 3T$.

We end with a few comments. It becomes evident that the late-time behavior of the system is highly sensitive to the spacing of the energy levels. The peaks occurring at later-time intervals are also increasingly shifted upward. For $\Delta > 0$, at some late time the subtle cancellations do not hold any longer and violent, chaotic behavior can occur due to the overlap of several contributions.

APPENDIX B: COUPLING TO TWO QUASICONTINUA

The evolution equations for a coupling to two quasicontinua $b_n(t)$ and $c_m(t)$ read

$$\dot{a}(t) = -i\sum_{n=-\infty}^{\infty}\beta_n^{(1)}b_n(t) - i\sum_{m=-\infty}^{\infty}\beta_m^{(2)}c_m(t), \quad (B1)$$

$$\dot{b}_n(t) = -i\omega_n^{(1)}b_n(t) - i\beta_n^{(1),*}a(t), \quad (B2)$$

$$\dot{c}_m(t) = -i\omega_m^{(2)}c_m(t) - i\beta_m^{(2),*}a(t), \quad (B3)$$

where the two energy levels are given by $\omega_n^{(i)} = n\Delta_i$ ($i = 1, 2$). The solution in Laplace space is given by

$$\tilde{a}(s) = \frac{a(0)}{s + \Pi_1(s) + \Pi_2(s)}, \quad (B4)$$

where $\Pi_j(s) = i\sum_{n=-\infty}^{\infty}|\beta_n^{(j)}|^2/(is - \omega_n^{(j)})$. We focus on the case of constant couplings, i.e., $\beta_n^{(i)} = \beta_i$. After, by now, standard manipulations we finally arrive at

$$\tilde{a}(s) = \frac{1}{s + \frac{\gamma_{12}}{2}}$$
$$- \sum_{k=1}^{\infty} \frac{\left[\left(s - \frac{\gamma_1}{2}\right)e^{-\tau_1 s} + \left(s - \frac{\gamma_2}{2}\right)e^{-\tau_2 s} - se^{-\tau_{12} s}\right]^{k-1}}{\left(s + \frac{\gamma_{12}}{2}\right)^{k+1}}$$
$$\times \left[\left(\gamma_1 + \frac{\gamma_2}{2}\right)e^{-\tau_1 s} + \left(\gamma_2 + \frac{\gamma_1}{2}\right)e^{-\tau_2 s} - \frac{\gamma_{12}}{2}e^{-\tau_{12} s}\right], \quad (B5)$$

where $\gamma_i = 2\pi|\beta_i|^2/\Delta_i$ and $\tau_i = 2\pi/\Delta_i$ and, finally, $\gamma_{12} = \gamma_1 + \gamma_2$ and $\tau_{12} = \tau_1 + \tau_2$. The amplitude picks again up new contributions at multiples of the revival times, and also allows arbitrary mixing between multiples of τ_1 and τ_2, e.g., $n\tau_1 \times m\tau_2$, and so forth. The first few terms in the expansion are

$$a_0(t) = e^{-t\gamma_{12}/2}, \quad (B6)$$

$$a_1(t) = -\left(\gamma_1 + \frac{\gamma_2}{2}\right)(t - \tau_1)e^{-(t-\tau_1)\gamma_{12}/2}\Theta(t - \tau_1)$$
$$- \left(\gamma_2 + \frac{\gamma_1}{2}\right)(t - \tau_2)e^{-(t-\tau_2)\gamma_{12}/2}\Theta(t - \tau_2)$$

$$+ \frac{\gamma_{12}}{2}(t - \tau_{12})e^{-(t-\tau_{12})\gamma_{12}/2}\Theta(t - \tau_{12}). \quad (B7)$$

At second order, we get contributions at revival times $t > 2\tau_1$, $2\tau_2$, τ_{12} and also $t > 2\tau_1 + \tau_2$, $\tau_1 + 2\tau_2$, $2\tau_{12}$. The former contributions are fully accounted for by the two first terms, while the latter will receive further contributions from the third term of the expansion. Let us therefore focus on the former for now. The contributions read

$$a_3(t) = -\left(\gamma_1 + \frac{\gamma_2}{2}\right)\left[(t - 2\tau_1) - \frac{1}{2}\left(\gamma_1 + \frac{\gamma_2}{2}\right)(t - 2\tau_1)^2\right]$$
$$\times e^{-(t-2\tau_1)\gamma_{12}/2}\Theta(t - 2\tau_1)$$
$$- \left(\gamma_2 + \frac{\gamma_1}{2}\right)\left[(t - 2\tau_2) - \frac{1}{2}\left(\gamma_2 + \frac{\gamma_1}{2}\right)(t - 2\tau_2)^2\right]$$
$$\times e^{-(t-2\tau_2)\gamma_{12}/2}\Theta(t - 2\tau_2)$$
$$- \left[\frac{3\gamma_{12}}{2}(t - \tau_{12}) - \left(\gamma_1 + \frac{\gamma_2}{2}\right)\left(\gamma_2 + \frac{\gamma_1}{2}\right)(t - \tau_{12})^2\right]$$
$$\times e^{-(t-\tau_{12})\gamma_{12}/2}\Theta(t - \tau_{12}). \quad (B8)$$

There are several distinct features that are worth pointing out.

The first peaks related to the revival times τ_i appear at times $t_i = \tau_i + 2/\gamma_{12}$ where the probability peaks at $|\frac{2\gamma_i + \gamma_j}{e\gamma_{12}}|^2$ (where γ_j refers to the other coupling, i.e., $i \neq j$), respectively. Strikingly, the height of these peaks depends on the couplings.

The revival time at $\tau_1 + \tau_2$ involves two peaks. The position and height of the peak can be found in a straightforward manner, but the expressions are complicated and not illuminating. Instead, focusing on the case when $\gamma_1 = \gamma_2 = \gamma$, we find that the revival times are located at $t = \tau_1 + \tau_2 + (13 \pm \sqrt{97})/(9\gamma)$ where the probability peaks at $|\frac{9 \pm \sqrt{97}}{2}e^{-(13 \pm \sqrt{97})/9}|^2$. Strikingly, this peak is again *not dependent* on the coupling. However, this statement does not hold for the general case when $\gamma_1 \neq \gamma_2$. We also repeat that these estimates only hold if the couplings are sufficiently large so that the previous revival peaks are completely washed out before the subsequent revival time.

As usual for constant coupling, double peaks also appear at multiples of the revival times τ_1 and τ_2, and also at their mixed multiples.

Finally, we can also find the occupation of the two bands, using Eq. (A3). In our case,

$$b_n(t) = \frac{i\beta_1}{\frac{\gamma_{12}}{2} - in\Delta_1}(e^{-t\gamma_{12}/2} - e^{-in\Delta_1 t}), \quad (B9)$$

and similarly for $c_n(t)$ by substituting $\beta_1 \to \beta_2$ and $\Delta_1 \to \Delta_2$. We define the probabilities:

$$P_b(t) = \sum_{n=-\infty}^{\infty}|b_n(t)|^2, \quad (B10)$$

$$P_c(t) = \sum_{n=-\infty}^{\infty}|c_n(t)|^2, \quad (B11)$$

and after some algebra, using Eqs. (A20) and (A21), we obtain Eq. (25), which proves that $P_a(t) + P_b(t) + P_c(t) = 1$.

[1] P. A. M. Dirac, Proc. R. Soc. A **114**, 243 (1927).

[2] L. Landau, Z. Phys. **45**, 430 (1927).

[3] V. F. Weisskopf and E. P. Wigner, Z. Phys. **63**, 54 (1930).

[4] F. L. Wilson, Am. J. Phys. **36**, 1150 (1968).

[5] E. Merzbacher, *Quantum Mechanics* (Wiley, New York, 1998).

[6] C. Rothe, S. I. Hintschich, and A. P. Monkman, Phys. Rev. Lett. **96**, 163601 (2006).

[7] M. Peshkin, A. Volya, and V. Zelevinsky, Europhys. Lett. **107**, 40001 (2014).

[8] N. G. Kelkar, M. Nowakowski, and K. P. Khemchandani, Phys. Rev. C **70**, 024601 (2004).

[9] G. Andersson, B. Suri, L. Guo, T. Aref, and P. Delsing, Nat. Phys. **15**, 1123 (2019).

[10] P. W. Milonni, J. R. Ackerhalt, H. W. Galbraith, and M.-L. Shih, Phys. Rev. A **28**, 32 (1983).

[11] C. Cohen-Tannoudji, J. Dupont-Roc, and G. Grynberg, *Atom-Photon Interactions: Basic Processes and Applications* (Wiley, New York, 1998).

[12] G. C. Stey and R. W. Gibberd, Physica **60**, 1 (1972).

[13] U. Fano, Il Nuovo Cimento (1924-1942) **12**, 154 (1935).

[14] W. A. Coish, J. Fischer, and D. Loss, Phys. Rev. B **77**, 125329 (2008).

[15] T. Micklitz, A. Morningstar, A. Altland, and D. A. Huse, Phys. Rev. Lett. **129**, 140402 (2022).

[16] L. Guo, A. Grimsmo, A. F. Kockum, M. Pletyukhov, and G. Johansson, Phys. Rev. A **95**, 053821 (2017).

[17] J. J. Yeh, C. M. Bowden, and J. H. Eberly, J. Chem. Phys. **76**, 5936 (1982).

[18] J. H. Eberly, N. B. Narozhny, and J. J. Sanchez-Mondragon, Phys. Rev. Lett. **44**, 1323 (1980).

[19] B. Gaveau and L. S. Schulman, J. Phys. A: Math. Gen. **28**, 7359 (1995).

[20] U. Fano, Phys. Rev. **124**, 1866 (1961).

[21] This discussion assumes that the revival peaks are completely suppressed when the next revival time sets in. In the opposite case one should expect further interference effects between contributions from different revival-time intervals.

[22] U. Dorner and P. Zoller, Phys. Rev. A **66**, 023816 (2002).

[23] This becomes clear from the simpler polynomial structure accompanying the exponentials in the sum.

[24] I. S. Gradshteyn and I. M. Ryzhik, *Table of Integrals, Series, and Products* (Academic, New York, 1965).